



Dynamics and Transport of the (Z_2) Spin Liquid: Application to $(\kappa\text{-}(\text{ET})_2\text{Cu}_2(\text{CN})_3)$

Citation

Qi, Yang, Cenke Xu, and Sachdev Subir. 2009. Dynamics and transport of the (Z_2) spin liquid: Application to $(\kappa\text{-}(\text{ET})_2\text{Cu}_2(\text{CN})_3)$. Physical Review Letters 102(17): 176401.

Published Version

doi:10.1103/PhysRevLett.102.176401

Permanent link

<http://nrs.harvard.edu/urn-3:HUL.InstRepos:7416455>

Terms of Use

This article was downloaded from Harvard University's DASH repository, and is made available under the terms and conditions applicable to Open Access Policy Articles, as set forth at <http://nrs.harvard.edu/urn-3:HUL.InstRepos:dash.current.terms-of-use#OAP>

Share Your Story

The Harvard community has made this article openly available.
Please share how this access benefits you. [Submit a story](#).

[Accessibility](#)

Dynamics and transport of the Z_2 spin liquid: application to κ -(ET) $_2$ Cu $_2$ (CN) $_3$

Yang Qi, Cenke Xu, and Subir Sachdev

Department of Physics, Harvard University, Cambridge MA 02138, USA

(Dated: September 2, 2008)

We describe neutron scattering, NMR relaxation, and thermal transport properties of Z_2 spin liquids in two dimensions. Comparison to recent experiments on the spin $S = 1/2$ triangular lattice antiferromagnet in κ -(ET) $_2$ Cu $_2$ (CN) $_3$ shows that this compound may realize a Z_2 spin liquid. We argue that the topological ‘vison’ excitations dominate thermal transport, and that recent thermal conductivity experiments by M. Yamashita *et al.* have observed the vison gap.

Much attention [1, 2, 3, 4, 5, 6, 7] has recently focused on the organic compound κ -(ET) $_2$ Cu $_2$ (CN) $_3$ because it may be the first experimental realization of a resonating valence bond spin liquid [8, 9]. This compound belongs to a class [10, 11] of organic Mott insulators which can be described by $S = 1/2$ spins residing on the vertices of a triangular lattice. Experiments have not detected any magnetic order or a structural distortion leading to a doubling of the unit cell in κ -(ET) $_2$ Cu $_2$ (CN) $_3$, and so there is justifiable optimism that the elusive spin liquid state may finally have been found.

The debate then turns to the identification of the precise spin liquid state, among the many possible candidates. Measurements of the electronic specific heat, C_P , by S. Yamashita *et al.* [3] were interpreted to yield a non-zero low temperature (T) value of $\gamma = \lim_{T \rightarrow 0} C_P/T$. Such a non-zero γ is characteristic of a Fermi surface, and hence a spin liquid state with a Fermi surface of neutral, $S = 1/2$, fermionic spinons was postulated [3, 5, 6]. However, it should be noted that the measurement of γ involves a potentially dangerous subtraction of a divergent nuclear specific heat [3].

Very recently, M. Yamashita *et al.* have measured [4] the thermal conductivity, κ , to below $T \approx 0.1$ K. This has the advantage of focusing on the mobile excitations, and not being contaminated by a nuclear contribution. A spinon Fermi surface should yield a non-zero low T limit for κ/T , but this quantity was clearly observed to vanish. Instead, the measured κ was fit reasonably well by the activated behavior $\kappa \sim \exp(-\Delta_\kappa/T)$, with a ‘gap’ $\Delta_\kappa \approx 0.46$ K. Furthermore, κ was found to be insensitive to an applied field for $H < 4$ T, suggesting that the gap Δ_κ is associated with a spinless excitation. These observations appear to be incompatible with spinon Fermi surface states at these low T , and we shall present an alternative theory here.

Also of interest are the measurements [2] of the NMR relaxation rate, $1/T_1$. The power-law behavior $1/T_1 \sim T^a$, with the exponent $a \approx 1.5$, was observed for $0.02 < T < 0.3$ K. This requires the presence of spinful excitations with a gapless spectrum at the fields of the NMR experiment, although at zero field there may well be a small spin gap.

In this paper, we will compare these observations with the Z_2 spin liquid state originally proposed in Refs. 12, 13, 14. The low energy excitations of this state are described by a Z_2 gauge theory, and the spinful excitations are constructed from $S = 1/2$ quanta (the spinons) which carry a Z_2 electric charge. Crucial to our purposes here are vortex-like spinless excitations [15] which carry Z_2 magnetic flux, later dubbed ‘visons’ [16]. A number of solvable models of Z_2 spin liquids, with spinon and vison excitations, have been constructed [16, 17, 18, 19, 20, 21, 22]. We propose here that it is the visons which dominate the thermal transport in κ -(ET) $_2$ Cu $_2$ (CN) $_3$, and the gap Δ_κ is therefore identified with a vison energy gap, Δ_v . If our interpretation is correct, the vison has been observed by M. Yamashita *et al.* [4].

Our proposal requires that the density of states of low energy vison excitations is much larger than that of all other excitations. A model appropriate to κ -(ET) $_2$ Cu $_2$ (CN) $_3$ is the triangular lattice $S = 1/2$ antiferromagnet with nearest neighbor two-spin exchange (J_2) and plaquette four-spin (J_4) exchange which was studied by Liming *et al.* [23]. They found antiferromagnetic order at $J_4 = 0$ (as in earlier work [24]), and a quantum phase transition to a spin liquid state with a spin gap around $J_4/J_2 \approx 0.1$. Notably, they found a very large density of low-lying spin singlet excitations near the transition. We propose here that κ -(ET) $_2$ Cu $_2$ (CN) $_3$ is near this quantum phase transition, and identify these singlets with visons which have a small gap and bandwidth, both much smaller than the spin exchange $J_2 \sim 250$ K. We will argue below that at $T \ll J_2$, and comparable to the vison bandwidth, visons will dominate the thermal transport.

Further support for the proximity of a magnetic ordering quantum critical point comes from [11] the closely related series of compounds X[Pd(dmit) $_2$] $_2$. By varying the anisotropy of the triangular lattice by varying X, we obtain compounds with decreasing magnetic ordering critical temperatures, until we eventually reach a compound with a spin gap and valence bond solid (VBS) order [25]. In between is the compound [27] with X=EtMe $_3$ P which has been proposed to be at the quantum critical point [11], and has properties similar to κ -(ET) $_2$ Cu $_2$ (CN) $_3$. Fi-

nally, series expansion studies [26] also place the triangular lattice antiferromagnet near a quantum critical point between magnetically ordered and VBS states.

A description of the NMR experiments requires a theory for the spinon excitations of the Z_2 spin liquid. The many models of Z_2 spin liquids [12, 13, 14, 15, 16, 17, 18, 19, 20, 21, 22] have cases with either fermionic or bosonic spinons. While we do not find a satisfactory explanation for the NMR with fermionic spinons, we show that a model [12, 13, 14] of bosonic spinons in a spin liquid close to the quantum phase transition to the antiferromagnetically ordered state (as found in the model of Liming *et al.* [23]) does naturally explain the T dependence of $1/T_1$. We shall show below that the quantum critical region for this transition leads to $1/T_1 \sim T^{\bar{\eta}}$ with the exponent [28, 29] $\bar{\eta} = 1.37$, reasonably close to the measured value $a = 1.5$. It is important to note that the vison gap, Δ_v , remains non-zero across this magnetic ordering critical point [35]. Consequently, our interpretation of the experiments remains valid even if the system acquires a small antiferromagnetic moment, as may be the case in the presence of the applied magnetic field present in the NMR measurements.

The remainder of the paper presents a number of computations of the physical properties of Z_2 spin liquids, and uses them to elaborate on the experimental interpretation sketched above.

We begin with a theory [30] of the spinon excitations near the quantum critical point between the magnetically ordered state and the Z_2 spin liquid. Here the low energy spinons are $S = 1/2$ complex bosons z_α , with $\alpha = \uparrow, \downarrow$ a spin index, and the low energy imaginary time action is

$$\mathcal{S} = \frac{1}{g} \int d^2r d\tau [|\partial_\tau z_\alpha|^2 + c^2 |\nabla_r z_\alpha|^2], \quad (1)$$

where (r, τ) are spacetime co-ordinates, g is a coupling which tunes the transition to the spin liquid present for some $g > g_c$, and c is a spin-wave velocity. We impose the local constraint $\sum_\alpha |z_\alpha|^2 = 1$ in lieu of a quartic self-interaction between the spinons. This theory has an emergent $O(4)$ global symmetry [29, 31] (which becomes manifest when z_α is written in terms of its real and imaginary components). This symmetry is an enlargement of the $SU(2)$ spin rotation symmetry, and we will neglect the irrelevant terms which reduce the symmetry to $SU(2)$.

(i) *Dynamic spin susceptibility.* The dynamic spin correlations of \mathcal{S} near the quantum critical point can be computed by the $1/N$ expansion on the $O(N)$ model, which has been described elsewhere [32]. With an eye towards possible future neutron scattering measurements, we first describe the dynamic spin susceptibility, $\chi(k, \omega)$ as a function of momentum k and real frequency ω . Here the momentum k is measured as a deviation from the ordering wavevector, Q , of the antiferromagnetically ordered state. At $g = g_c$ and $T = 0$, this has the quantum-

critical form

$$\chi(k, \omega) = \frac{\mathcal{A}}{(c^2 k^2 - \omega^2)^{1-\bar{\eta}/2}}, \quad (2)$$

where the exponent $\bar{\eta}$ is related to the scaling dimension of the composite spin operator $\sim z_\alpha \sigma_{\alpha\gamma}^y \vec{\sigma}_{\gamma\beta} z_\beta$ ($\vec{\sigma}$ are the Pauli matrices), and is known with high precision from field-theoretic studies [28] ($\bar{\eta} = 1.374(12)$) and Monte Carlo simulations [29] ($\bar{\eta} = 1.373(2)$). The overall amplitude \mathcal{A} is non-universal, but the same \mathcal{A} will appear in a number of results below. Integrating Eq. (2) over all k , we obtain the local susceptibility $\chi_L(\omega)$, which is also often measured in scattering experiments, again at $g = g_c$ and $T = 0$

$$\text{Im } \chi_L(\omega) = \frac{\mathcal{A} \text{sgn}(\omega) \sin(\pi\bar{\eta}/2)}{4c^2 \pi\bar{\eta}/2} |\omega|^{\bar{\eta}}. \quad (3)$$

Let us now move into the spin liquid state, with $g > g_c$, where the spinons have an energy gap Δ_z . The critical results in Eqs. (2) and (3) will apply for $|\omega| \gg \Delta_z$, but for $|\omega| \sim 2\Delta_z$, we will have spectra characteristic of the creation of a pair of spinons (we set $\hbar = 1$, although it appears explicitly in a few expressions below). Computing the pair creation amplitude of non-interacting spinons, we obtain a step-discontinuity threshold at $\omega = \sqrt{c^2 k^2 + 4\Delta_z^2}$ (at $T = 0$). However, the spinons do have a repulsive interaction with each other, and this reduces the phase space for spinon creation at low momentum, as described in the supplementary material; the actual threshold behavior is:

$$\text{Im } \chi(k, \omega) = \frac{\mathcal{A} \mathcal{C} \text{sgn}(\omega)}{\Delta_z^{2-\bar{\eta}}} \frac{\theta\left(|\omega| - \sqrt{k^2 + 4\Delta_z^2}\right)}{\ln^2\left(\frac{|\omega^2 - k^2 - 4\Delta_z^2|}{16\Delta_z^2}\right)}, \quad (4)$$

where \mathcal{C} is a universal constant; to leading order in the $1/N$ expansion, $\mathcal{C} = N^2/16$. We can also integrate the k -dependent generalization of Eq. (4) to obtain a threshold behavior for the local susceptibility at $2\Delta_z$: $\text{Im } \chi_L(\omega) \sim \text{sgn}(\omega)(|\omega| - 2\Delta_z)/\ln^2(|\omega| - 2\Delta_z)$.

(ii) *NMR relaxation.* Turning to the NMR relaxation rate, we have to consider $T > 0$, and compute

$$\Gamma = \lim_{\omega \rightarrow 0} \frac{k_B T}{\omega} \text{Im } \chi_L(\omega). \quad (5)$$

This is far more subtle than the computations at $T = 0$, because we have to compute the damping of the quantum critical excitations at $T > 0$ and extend to the regime $\omega \ll T$. From general scaling arguments [32], we have

$$\Gamma = \frac{\mathcal{A}}{c^2} (k_B T)^{\bar{\eta}} \Phi(\Delta_z/(k_B T)), \quad (6)$$

where Φ is a universal function. The computation of Φ for undamped spinons at $N = \infty$ is straightforward,

and unlike the case for confining antiferromagnets [32], yields a reasonable non-zero answer: $\Phi(y) = [4\pi e^{y/2}(1 + \sqrt{4 + e^y})]^{-1}$. However, the $1/N$ corrections are singular, because Γ has a singular dependence upon the spinon lifetime. A self-consistent treatment of the spinon damping is described in the supplementary material, and leads to the quantum-critical result ($\Delta_z = 0$):

$$\Phi(0) = \frac{(\sqrt{5} - 1)}{16\pi} \left(1 + 0.931 \frac{\ln N}{N} + \dots \right). \quad (7)$$

(iii) *Thermal conductivity.* We now turn to the thermal transport co-efficient measured in the recent revealing experiments of Ref. 4. We consider the contribution of the spinons and visons in turn below, presenting further arguments on why the vison contribution can dominate in the experiments.

(iii.a) *Spinons.* For agreement with the NMR measurements of $1/T_1$ [2], we need the spinons to be in the quantum critical regime, as described above. Therefore, we limit our considerations here to the quantum critical thermal conductivity of the spinons, κ_z , with $\Delta_z = 0$. This can be obtained from the recent general theory of quantum critical transport [33] which yields

$$\kappa_z = s c^2 \tau_z^{\text{imp}}, \quad (8)$$

where s is the entropy density of the spinons, and $1/\tau_z^{\text{imp}}$ is the spinon momentum relaxation rate, with the T dependence

$$\tau_z^{\text{imp}} \sim T^{2/\nu-3}. \quad (9)$$

Here ν is the critical exponent of the O(4) model [34], $\nu = 0.749(2)$, and so $\tau_z^{\text{imp}} \sim T^{-0.33}$. The two dimensional entropy density can be obtained from the results of Ref. 32:

$$s = \frac{3N\zeta(3)k_B^3 T^2}{2\pi\hbar^2 c^2} \left[\frac{4}{5} - \frac{0.3344}{N} + \dots \right], \quad (10)$$

where ζ is the Reimann zeta function. We estimate the co-efficient in Eq. (9) in the supplementary material using a soft-spin theory with the spinons moving in a random potential, $V(r)|z_\alpha|^2$, due to impurities of density n_{imp} each exerting a Yukawa potential $V_q = V_z/(q^2 + \mu^2)$; this leads to

$$\kappa_z \sim \frac{Nc^2\hbar k_B^4 \mu^4 T^2 T_z}{an_{\text{imp}}V_z^2} \times \left(\frac{T}{T_z} \right)^{2/\nu-3}. \quad (11)$$

Here a is the spacing between the layers, and T_z is the spinon bandwidth in temperature units and is proportional to the spinon velocity c .

(iii.b) *Visons.* The visons are thermally excited across an energy gap, Δ_v , and so can be considered to be a dilute Boltzmann gas of particles of mass m_v . We assume there are N_v species of visons. The visons see the

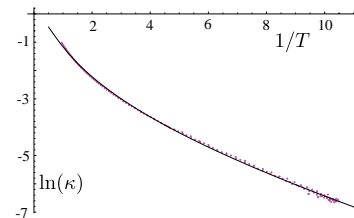


FIG. 1: Fit of the T dependence of the vison thermal conductivity in Eq. (12) to the thermal conductivity measurements by Yamashita *et al.* [4]; T_v , Δ_v and the overall prefactor were the fit parameters.

background filling of spins as a magnetic flux through the plaquette on the dual lattice, and hence the dynamics of visons can be well described by a fully-frustrated quantum Ising model on the honeycomb lattice. Detailed calculations show that there are four minima of the vison band with an emergent O(4) flavor symmetry at low energy [17], therefore $N_v = 4$. As with the spinons, the visons are assumed to scatter off impurities of density n_{imp} with, say, a Yukawa potential $V_q = V_v/(q^2 + \mu^2)$. We use the fact that at low T , and for a large vison mass m_v , the visons are slowly moving. So each impurity scattering event can be described by a T -matrix $= [m_v \ln(1/k)/\pi]^{-1}$ characteristic of low momentum scattering in two dimensions. Application of Fermi's golden rule then yields a vison scattering rate $1/\tau_v^{\text{imp}} = \pi^2 n_{\text{imp}} / (m_v \ln^2(1/k))$. This formula becomes applicable when $\ln(1/k) \times V_v / (\hbar^2 \mu^2 / 2m_v) \gg 1$ *i.e.* the impurity potential becomes nonperturbative. We can now insert this scattering rate into a standard Boltzmann equation computation of the thermal conductivity $\kappa_v = 2k_B^2 T n_v \tau_v^{\text{imp}} / m_v$, where n_v is the thermally excited vison density and the typical momentum $k \sim (m_v k_B T)^{1/2}$, to obtain

$$\kappa_v = \frac{N_v m_v k_B^3 T^2 \ln^2(T_v/T) e^{-\Delta_v/(k_B T)}}{4\pi\hbar^3 n_{\text{imp}} a}. \quad (12)$$

Here T_v is some ultraviolet cutoff temperature which can be taken as the vison bandwidth. Note that for a large density of states of vison excitations, *i.e.* a large m_v , the prefactor of the exponential can be large. Similar calculations will not lead to a logarithmic divergence for the critical spinon z due to the positive anomalous dimension of $|z|^2$, and therefore the impurity scattering of spinons is perturbative for $V_z/(c\mu\hbar)^2 < 1$.

Using Eq. (12), we fit the thermal conductivity measured by M. Yamashita *et al.* in Ref. 4 by tuning parameters T_v and Δ_v . The best fit values are $T_v = 8.15K$, and $\Delta_v \equiv \Delta_\kappa = 0.238K$, as shown in Fig. 1. For consistency check, we calculate the ratio between the thermal conductivities contributed by spinons and visons using Eq. (11) and Eq. (12) and assuming moderate spinon

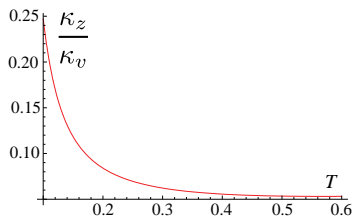


FIG. 2: Ratio of the thermal conductivity of spinons to visons in Eq. (13)

impurity strength $V_z/(c\mu\hbar)^2 \sim 1$:

$$\begin{aligned} \frac{\kappa_z}{\kappa_v} &\sim \frac{k_B T_z}{m_v c^2} \times \left(\frac{T}{T_z}\right)^{2/\nu-3} \frac{1}{(\ln T_v/T)^2} e^{\Delta_v/k_B T} \\ &\sim \frac{T_v}{T_z} \times \left(\frac{T}{T_z}\right)^{2/\nu-3} \frac{1}{(\ln T_v/T)^2} e^{\Delta_v/(k_B T)}. \end{aligned} \quad (13)$$

We plot this ratio in Fig. 2, with $T_z \sim J_2 = 250$ K and other parameters as above, for the experimentally relevant temperature between 0.1 K and 0.6 K; we find consistency because κ is dominated by the vison contribution. The vison dispersion is quadratic above the vison gap, and this leads to a T -independent $\gamma = C_p/T$ when $T > \Delta_v$, as observed in experiments [3]. Our estimate of the vison bandwidth, T_v , is also consistent with a peak in both C_p [3] and κ [4] at a temperature close to T_v .

The vison gap, Δ_v , obtained here is roughly the same as the temperature at which the $1/T_1$ of NMR starts to deviate from the low temperature scaling of Eq. (6) [2]. When T is above Δ_v , thermally activated visons will proliferate. We discuss a theory of the spin dynamics in this thermal vison regime in the supplement, and find a $1/T_1$ with a weaker T dependence compared to that present for $T < \Delta_v$. These observations are qualitatively consistent with the NMR data for $0.25 < T < 10$ K [2].

Ref. 4 also measured the thermal conductivity, in an applied field H up to 10 T. There was little change in κ for $H < 4$ T. As H couples to the conserved total spin, it only appears as an opposite “chemical potential” term for z_α , modifying the temporal derivative $(\partial_\tau + (H/2)\sigma^z)z^\dagger(\partial_\tau - (H/2)\sigma^z)z$. At the quantum critical point, this term will induce a condensate of z *i.e.* a non-collinear magnetically ordered state. We do not expect a significant difference in the thermal conductivity of the gapless spinons versus gapless spin-waves across this second order transition. We conjecture that the change at 4 T is associated with a vison condensation transition to a valence bond solid, as the field scale is or order the energy scales noted in the previous paragraph. This transition is possibly connected to the H -dependent broadening of the NMR spectra [2].

We have described the properties of a Z_2 spin liquid, on the verge of a transition to an magnetically ordered state, We have argued that the quantum critical spinons describe the NMR observations [2], while the visons (with

a small energy gap and bandwidth) dominate the thermal transport [4].

We are very grateful to Minoru Yamashita for valuable discussions of the results of Ref. 4, and to the authors of Ref. 4 for permission to use their data in Fig. 1. We thank K. Kanoda, S. Kivelson, and T. Senthil for useful discussions. This research was supported by the NSF under grant DMR-0757145.

-
- [1] Y. Shimizu *et al.*, Phys. Rev. Lett. **91**, 107001 (2003).
 - [2] Y. Shimizu *et al.*, Phys. Rev. B **73**, 140407(R) (2006).
 - [3] S. Yamashita *et al.*, Nature Physics **4**, 459 (2008).
 - [4] M. Yamashita *et al.*, Nature Physics **5**, 44 (2008).
 - [5] O. I. Motrunich, Phys. Rev. B **72**, 045105 (2005).
 - [6] S.-S. Lee, P. A. Lee, and T. Senthil, Phys. Rev. Lett. **98**, 067006 (2007).
 - [7] Y. Qi and S. Sachdev, Phys. Rev. B **77**, 165112 (2008).
 - [8] P. Fazekas and P. W. Anderson, Philos. Mag. **30**, 23 (1974).
 - [9] S. A. Kivelson, D. S. Rokhsar, and J. P. Sethna, Phys. Rev. B **35**, 8865 (1987).
 - [10] B. J. Powell and R. H. McKenzie, J. Phys.: Condens. Matter **18**, R827 (2006).
 - [11] Y. Shimizu *et al.*, J. Phys.: Condens. Matter **19**, 145240 (2007).
 - [12] N. Read and S. Sachdev, Phys. Rev. Lett. **66**, 1773 (1991).
 - [13] R. Jalabert and S. Sachdev, Phys. Rev. B **44**, 686 (1991).
 - [14] S. Sachdev, Phys. Rev. B **45**, 12377 (1992).
 - [15] N. Read and B. Chakraborty, Phys. Rev. B **40**, 7133 (1989).
 - [16] T. Senthil and M. P. A. Fisher, Phys. Rev. B **63**, 134521 (2001).
 - [17] R. Moessner and S. L. Sondhi, Phys. Rev. B **63**, 224401 (2001).
 - [18] A. Y. Kitaev, Annals of Physics **303**, 2 (2003).
 - [19] X. G. Wen, Phys. Rev. B **44**, 2664 (1991); Phys. Rev. Lett. **90**, 016803 (2003).
 - [20] M. Freedman *et al.*, Annals of Physics **310**, 428 (2004).
 - [21] F. Wang and A. Vishwanath, Phys. Rev. B **74**, 174423 (2006).
 - [22] G. Misguich and F. Mila, Phys. Rev. B **77**, 134421 (2008).
 - [23] W. LiMing *et al.*, Phys. Rev. B **62**, 6372 (2000).
 - [24] R. R. P. Singh and D. A. Huse, Phys. Rev. Lett. **68**, 1766 (1992).
 - [25] M. Tamura, A. Nakao and R. Kato, J. Phys. Soc. Japan **75**, 093701 (2006); Y. Shimizu *et al.*, Phys. Rev. Lett. **99**, 256403 (2007).
 - [26] Z. Weihong, R. H. McKenzie, and R. R. P. Singh, Phys. Rev. B **59**, 14367 (1999).
 - [27] T. Itou, A. Oyamada, S. Maegawa, M. Tamura, and R. Kato, Phys. Rev. B **77**, 104413 (2008).
 - [28] P. Calabrese, A. Pelissetto, and E. Vicari, Phys. Rev. B **67**, 054505 (2003).
 - [29] S. V. Isakov, T. Senthil, and Y. B. Kim, Phys. Rev. B **72**, 174417 (2005).
 - [30] A. V. Chubukov, T. Senthil and S. Sachdev, Phys. Rev. Lett. **72**, 2089 (1994).
 - [31] P. Azaria, B. Delamotte, and T. Jolicoeur, Phys. Rev. Lett. **64**, 3175 (1990).
 - [32] A. V. Chubukov, S. Sachdev, and J. Ye, Phys. Rev. B

- 49**, 11919 (1994).
- [33] S. A. Hartnoll *et al.*, Phys. Rev. B **76**, 144502 (2007);
M. Müller and S. Sachdev, Phys. Rev. B **78**, 115419 (2008)
- [34] M. Hasenbusch, J. Phys. A **34**, 8221 (2001).
- [35] In the ordered state, the visons have a logarithmic interaction, and the self-energy of an isolated vison diverges logarithmically with system size

Dynamics and transport of the Z_2 spin liquid: application to κ -(ET) $_2$ Cu $_2$ (CN) $_3$

Supplementary information.

Yang Qi, Cenke Xu, and Subir Sachdev

Department of Physics, Harvard University, Cambridge MA 02138, USA

(Dated: February 3, 2009)

This supplement presents additional details on computations in the main text. The large N expansion of the nonlinear σ model field theory of the transition between the Z_2 spin liquid and the phase with non-collinear magnetic order is presented in Section I. The thermal conductivity of the spinons is considered in Section II, and the NMR relaxation rate at temperatures above the vison gap is discussed in Section III.

I. LARGE- N EXPANSION OF NONLINEAR σ MODEL

The phase transition between a non-collinear Néel state and spin liquid state can be described by the O(4) nonlinear σ model as in Eq. (1) in the main text

$$S = \frac{1}{g} \int d^2r d\tau [|\partial_\tau z_\alpha|^2 + c^2 |\nabla_r z_\alpha|^2], \quad (1)$$

with the constraint that $|z_1|^2 + |z_2|^2 = 1$. The physical antiferromagnetic order parameter is related to the O(4) field z_α by the bilinear function [1, 2]

$$S^i = z_\alpha \sigma_{\alpha\gamma}^y \sigma_{\gamma\beta}^i z_\beta. \quad (2)$$

This differs from the collinear case, where the order parameter is linearly proportional to the field of the O(3) σ model. Therefore, the spin correlation function is proportional to a bubble diagram of the z field (see Fig. 1) [1]:

$$\chi(x, \tau) \sim \Pi(x, \tau) = \langle z_\alpha(x, \tau) z_\beta(x, \tau) z_\beta^*(0, 0) z_\alpha^*(0, 0) \rangle. \quad (3)$$

The correlation function $\Pi(k, \omega)$ for the O(4) field can then be calculated using the large- N expansion. The framework of the expansion can be set up in the disordered phase as follows. First, we rewrite the constraint as a path integral over a Lagrangian multiplier field λ

$$S = \frac{N}{2g} \int d^2r d\tau [|\partial_\tau z_\alpha|^2 + c^2 |\nabla_r z_\alpha|^2 + i\lambda(|z_\alpha|^2 - 1)]. \quad (4)$$

Here the coupling constant g is rescaled from that in Eq. (1) in the main text to show the N dependence in the large- N limit explicitly. Integrating out the n field

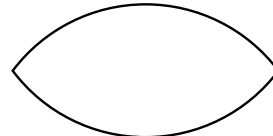


FIG. 1: Bubble diagram for the correlation function of Π . The solid line represents propagator given by equation (8).

in the above action, the path integral over λ becomes

$$\mathcal{Z} = \int \mathcal{D}\lambda \exp \left[-\frac{N}{2} \left(\text{Tr} \ln(-c^2 \nabla^2 - \partial_\tau^2 + i\lambda) - \frac{i}{g} \int d\tau d^2x \lambda \right) \right]. \quad (5)$$

Therefore, in the $N \rightarrow \infty$ limit, the path integral is dominated by the contribution from the classical path, along which λ becomes a constant given by the saddle point equation

$$\frac{1}{\beta} \sum_{\omega_n} \int \frac{d^2k}{(2\pi)^2} \frac{1}{\omega_n^2 + c^2 k^2 + m^2} = \frac{1}{g}, \quad (6)$$

where $m^2 = i\lambda$, and $m = \Delta_z^{(0)}$ is the spinon gap in the $N \rightarrow \infty$ limit.

At the $N = \infty$ order, the λ field is treated as a constant, and the theory contains only free z_α field with mass gap Δ_z . The full large- N expansion is obtained by including fluctuations of λ controlled by the action in Eq. (5): the N^{-n} order expansion corresponds to a n -loop correction.

The spin correlation function in Eq. (3) can be calculated from the $\Pi(\mathbf{k}, \omega)$ correlation function for the z_α field using the large- N expansion. At $N = \infty$ order, the correlation function is given by a bubble diagram of two free propagators,

$$\Pi_0(k, i\omega_n) = \int \frac{d^2p}{(2\pi)^2} \frac{1}{\beta} \sum_{\nu_n} G_0(\mathbf{p}, i\nu_n) G_0(\mathbf{p} + \mathbf{k}, i\nu_n + i\omega_n), \quad (7)$$

where $G_0(p, i\omega_n)$ is the free propagator of z_α field

$$G_0(p, i\omega_n) = \frac{1}{c^2 p^2 + \omega_n^2 + m^2}. \quad (8)$$

At the $1/N$ order, the contribution from the fluctuation of the λ field needs to be included at one-loop level. There are two corrections that need to be included for the bubble diagram: the self-energy correction and the vertex correction.

First, the bare propagator in Eq. (7) needs to be replaced by a propagator with a self-energy correction at one-loop level[3].

$$G(k, i\omega_n) = \frac{1}{\omega_n^2 + c^2 k^2 + m^2 + \Sigma(k, i\omega_n)}, \quad (9)$$

where the self-energy has two parts. The first part comes from an insertion of λ propagator on z_α propagator shown in Fig. 2:

$$\tilde{\Sigma}(k, i\omega_n) = \frac{2}{N} \frac{1}{\beta} \sum_{\nu_n} \int \frac{d^2 p}{(2\pi)^2} \frac{G_0(\mathbf{k} + \mathbf{q}, i\omega_n + i\nu_n) - G_0(k, i\omega_n)}{\Pi_0(q, i\nu_n)}. \quad (10)$$

The second contribution is given by Fig. 3, and the total self-energy is

$$\Sigma(k, i\omega_n) = \tilde{\Sigma}(k, i\omega_n) - \frac{1}{\Pi_0(0, 0)} \frac{1}{\beta} \sum_{\nu_n} \int \frac{d^2 p}{(2\pi)^2} G_0(p, i\nu) \tilde{\Sigma}(k, i\nu_n) G_0(p, i\nu_n). \quad (11)$$

In addition to including the self-energy in the propagators of $\Pi(k, i\omega_n)$, the vertex correction (see Fig. 4) also needs to be included.

$$\Pi^{(1v)}(k, i\omega_n) = \frac{2}{N} \frac{1}{\beta^2} \sum_{\nu_n, \epsilon_n} \int \frac{d^2 p d^2 q}{(2\pi)^4} \frac{G_0(p, i\nu_n) G_0(\mathbf{p} + \mathbf{q}, i\nu_n + i\epsilon_n) G_0(\mathbf{p} + \mathbf{k}, i\nu_n + i\omega_n) G_0(\mathbf{p} + \mathbf{q} + \mathbf{k}, i\nu_n + i\epsilon_n + i\omega_n)}{\Pi_0(q, i\epsilon_n)}. \quad (12)$$

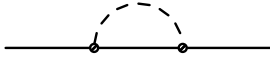


FIG. 2: The first term in self-energy correction: $\tilde{\Sigma}(k, i\omega_n)$ evaluated in equation (10). In this diagram and Fig. 3 the dotted line represents propagator of λ field given in equation (5), and interaction vertex between two z_α field operators and one λ field operator is given by the last term in action (4).

A. Local susceptibility

In this section we consider the behavior of the imaginary part of dynamical susceptibility at the threshold to creating two spinon excitations. At $N = \infty$ and zero temperature, the integral in the expression of $\Pi(k, i\omega_n)$ can be evaluated analytically from Eq. (7), and the result is

$$\Pi_0(k, \omega) = \frac{1}{4\pi\sqrt{c^2 k^2 - \omega^2}} \tan^{-1} \left(\frac{\sqrt{c^2 k^2 - \omega^2}}{2m} \right). \quad (13)$$

The real and imaginary part of above equation have the following asymptotic behavior when ω is just above the

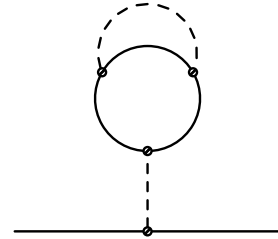


FIG. 3: The second term in self-energy correction, which corresponds to the last term of equation (11). This diagram contains two λ fields, which scales as N^{-2} , and also a loop of z_α field, which contributes a factor of N . Therefore the whole diagram is also at the order of $1/N$.

threshold

$$\text{Re } \Pi_0(k, \omega) = \frac{1}{16\pi m} \ln \left(\frac{\omega^2 - c^2 k^2 - 4m^2}{16m^2} \right), \quad (14)$$

and

$$\text{Im } \Pi_0(k, \omega) = \frac{\text{sgn}(\omega)}{8\sqrt{\omega^2 - c^2 k^2}} \theta(\omega - \sqrt{c^2 k^2 + 4m^2}). \quad (15)$$

Naturally, Eqs (14) and (15) are connected by a Kramers-Kronig relation.

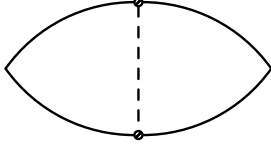


FIG. 4: Vertex correction for the bubble diagram, appeared in equation (12).

The sharp discontinuity in the imaginary part of susceptibility is an artifact of the $N = \infty$ limit, and is modified once we add in vertex corrections. Actually, as the bubble diagram evaluated in equation (13) has a logarithmic divergence at the threshold, the ladder diagrams, which contains all orders of this divergence, should be summed as in an RPA approximation (see Fig. 5). Since the bubble is divergent at the threshold, the most divergent contribution to the ladder diagrams comes from the propagator that is on shell and at the spinon threshold. When that happens, there is no momentum transfer through the λ propagator. Therefore, we can approximate the interaction vertex in the RPA summation as the λ propagator at zero momentum:

$$u = \frac{2}{N} \frac{1}{\Pi_0(0,0)} = \frac{16\pi}{N} m. \quad (16)$$

Therefore the RPA resummation of the ladder diagrams

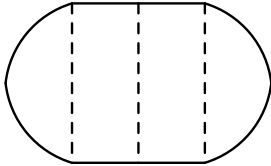


FIG. 5: Ladder diagram for vertex correction. A RPA resummation of these diagrams is evaluated in equation (16).

gives

$$\Pi = \Pi_0 + \Pi_0 u \Pi_0 + \dots = \frac{\Pi_0}{1 - u \Pi_0}. \quad (17)$$

Taking the imaginary part of χ , and taking only the most divergent part, we obtain

$$\text{Im} \Pi = \frac{\text{Im} \Pi_0}{u^2 (\text{Re} \Pi_0)^2}. \quad (18)$$

Plugging into Eqs (14) and (15), we obtain

$$\text{Im} \Pi(k, \omega) = \frac{N^2 \text{sgn}(\omega)}{8\sqrt{\omega^2 - c^2 k^2}} \frac{\theta(|\omega| - \sqrt{c^2 k^2 + 4m^2})}{\ln^2\left(\frac{\omega^2 - c^2 k^2 - 4m^2}{16m^2}\right)}. \quad (19)$$

In order to relate this result for Π to the physical spin correlation function χ , we need to insert the proportional constant in Eq. (3). Combined with the spectral weight from higher loop corrections, this gives the constant \mathcal{A} appearing in Eq. (2) in the main text. The mass gap of the spinon $\Delta_z^0 = m$ also receives higher loop corrections and becomes Δ_z in general. In addition, near the threshold, the factor of $\sqrt{\omega^2 - c^2 k^2}$ is approximately $2\Delta_z$. Therefore the above equation can be rearranged into

$$\text{Im} \chi(k, \omega) = \frac{\mathcal{A} N^2 \text{sgn}(\omega)}{16\Delta_z} \frac{\theta\left(|\omega| - \sqrt{c^2 k^2 + 4\Delta_z^2}\right)}{\ln^2\left(\frac{\omega^2 - c^2 k^2 - 4\Delta_z^2}{16\Delta_z^2}\right)}. \quad (20)$$

The overall scaling $\text{Im} \chi \sim \Delta_z^{-1}$ is a result at $N = \infty$, and shall be refined to $\text{Im} \chi \sim \Delta_z^{2-\bar{\eta}}$ when higher loop corrections are included, where $\bar{\eta}$ is the scaling component appearing in Eq. (2) in the main text. With this correction, the above equation becomes

$$\text{Im} \chi(k, \omega) = \frac{\mathcal{A} N^2 \text{sgn}(\omega)}{16\Delta_z^{2-\bar{\eta}}} \frac{\theta\left(|\omega| - \sqrt{c^2 k^2 + 4\Delta_z^2}\right)}{\ln^2\left(\frac{\omega^2 - c^2 k^2 - 4\Delta_z^2}{16\Delta_z^2}\right)}, \quad (21)$$

which is the same as Eq. (4) in the main text with $\mathcal{C} = N^2/16$.

B. Relaxation rate at order $1/N$

In this section we calculate the relaxation rate at $1/N$ order, at finite temperature above the critical point. We will show that, in the leading order of $1/N$ expansion, there is a singular term proportional to $\ln N/N$.

Following Eq. (5) in the main text, we calculate

$$\Gamma = \lim_{\omega \rightarrow 0} \frac{1}{\omega} \int \frac{d^2 q}{(2\pi)^2} \text{Im} \chi_L(q, \omega). \quad (22)$$

The singularity arises from the $1/N$ self-energy, by replacing χ_L with Π calculated with the full Green's function in Eq. (9).

$$\Pi(q, i\omega_n) = \int \frac{d^2 k}{(2\pi)^2} \sum_{\nu_n} G(k, i\nu_n) G(\mathbf{k} + \mathbf{q}, i\nu_n + i\omega_n). \quad (23)$$

In the critical region, temperature is the only energy scale. Therefore we have set $\beta = 1$ in the above equation, and in the remainder of this subsection.

Plugging Eq. (23) into (22), we obtain

$$\Gamma = \lim_{\omega \rightarrow 0} \frac{1}{\omega} \int \frac{d^2 q d^2 k}{(2\pi)^4} \sum_{\nu_n} \text{Im} G(k, i\nu_n) G(\mathbf{k} + \mathbf{q}, i\nu_n + i\omega_n). \quad (24)$$

Using the frequency summation identity

$$\begin{aligned} \lim_{\omega \rightarrow 0} \frac{1}{\omega} \text{Im} \sum_{\nu_n} G_1(i\nu_n) G_2(i\nu_n + i\omega_n) \\ = \int_{-\infty}^{\infty} \frac{d\epsilon}{2\pi} \frac{\text{Im} G_1(\epsilon) \text{Im} G_2(\epsilon)}{2 \sinh^2 \frac{\epsilon}{2}}, \end{aligned} \quad (25)$$

and changing the variable in the second integral from q to $\mathbf{k} + \mathbf{q}$, we obtain

$$\Gamma = \int_{-\infty}^{\infty} \frac{d\epsilon}{2\pi} \frac{A(\epsilon)^2}{2 \sinh^2 \frac{\epsilon}{2}}, \quad (26)$$

where

$$A(\epsilon) = \int \frac{d^2 k}{(2\pi)^2} \text{Im} G(k, \epsilon), \quad (27)$$

and the Green's function includes self-energy correction at $1/N$ order

$$G(k, \omega) = \frac{1}{c^2 k^2 + m^2 - \omega^2 + \Sigma(k, \omega)}. \quad (28)$$

Below we will see that the imaginary part of the self-energy leads to a $\ln N/N$ term, which is more divergent than the $1/N$ correction from the real part. So if we ignore the real part of the self-energy for the moment, the imaginary part of Green's function is

$$\text{Im} G(k, \omega) = \frac{\text{Im} \Sigma(k, \omega)}{(c^2 k^2 + m^2 - \omega^2)^2 + [\text{Im} \Sigma(k, \omega)]^2}, \quad (29)$$

where $\Sigma(k, \omega)$ is of order $1/N$. For the case that $k^2 + m^2 - \omega^2 \neq 0$, the integrand can be expanded to the order of $1/N$ by ignoring the $\text{Im} \Sigma$ term in the denominator. Therefore, we expand $\text{Im} \Sigma$ around the quasiparticle pole $ck_0 = \sqrt{\omega^2 - m^2}$:

$$\begin{aligned} \Sigma(k, \omega) &= \Sigma(k_0, \omega) \\ &+ \Sigma'(k_0, \omega)(k^2 - k_0^2) + O((k^2 - k_0^2)^2); \end{aligned} \quad (30)$$

the integral of the second term does not have a singularity because $k^2 - k_0^2$ is an odd function, and higher order terms are also not singular. Hence these terms result in regular corrections of the order $1/N$. However, integrating the constant term is divergent near the pole if the $\text{Im} \Sigma$ term is ignored. Therefore it needs to be put back and the most divergent term in $A(\omega)$ is

$$A(\omega) \sim \int \frac{d^2 k}{(2\pi)^2} \frac{\text{Im} \Sigma(k_0, \omega)}{c^2 (k - k_0)^2 + [\text{Im} \Sigma(k_0, \omega)]^2}, \quad (31)$$

and the result of this integral is

$$A(\omega) \sim \frac{1}{8c^2} + \frac{1}{4\pi c^2} \arctan \left[\frac{\omega^2 - m^2}{\text{Im} \Sigma(\sqrt{\omega^2 - m^2}, \omega)} \right]. \quad (32)$$

The function $A(\omega)$ can be expanded to the first two orders of $\text{Im} \Sigma$ as

$$A(\omega) \sim \frac{1}{4c^2} - \frac{1}{4\pi c^2} \frac{\text{Im} \Sigma(\sqrt{\omega^2 - m^2}, \omega)}{\omega^2 - m^2}. \quad (33)$$

Plugging this into Eq. (26), we obtain

$$\begin{aligned} \Gamma &= \frac{1}{c^2} \int_m^{\infty} \frac{d\epsilon}{2\pi} \frac{1}{\sinh^2(\epsilon/2)} \\ &\times \left[\frac{1}{16} - \frac{1}{8\pi} \frac{\text{Im} \Sigma(\sqrt{\epsilon^2 - m^2}, \omega)}{\epsilon^2 - m^2} \right]. \end{aligned} \quad (34)$$

The first term resembles the relaxation rate in the $N = \infty$ limit, and the second term yields a $1/(N \ln N)$ correction because the integrand diverges when $\epsilon \rightarrow m$

$$\Gamma^{(1)} \sim \frac{1}{16\pi^2 c^2} \frac{\text{Im} \Sigma(0, m)}{2m \sinh^2(m/2)} \ln \text{Im} \Sigma(0, m). \quad (35)$$

Here m is the mass gap of spinon in the critical region at $\beta = 1$. In the $N = \infty$ limit it can be evaluated analytically

$$m = \Theta = 2 \ln \frac{\sqrt{5} + 1}{2}.$$

At order $1/N$ it has been calculated that[4]

$$\frac{1}{\tau} = -\frac{\text{Im} \Sigma(0, m)}{2m} = \frac{0.904}{N}.$$

Thus we obtain

$$\begin{aligned} \Gamma^{(1)} &\sim \frac{0.904}{16\pi^2 c^2 \sinh^2 \Theta/2} \frac{1}{N} \ln N \\ &= \frac{\sqrt{5} - 1}{16\pi c^2} 0.931 \frac{\ln N}{N}. \end{aligned} \quad (36)$$

This is the $\ln N/N$ correction in Eq. (7) in the main text.

II. SPINON THERMAL CONDUCTIVITY

The general equation for thermal conductivity at 2+1d CFT was given in Eq. 8 in the paper:

$$\kappa_z = s c^2 \tau_{\text{imp}}. \quad (37)$$

The entropy density s is given in the paper by Eq. (10). Based on simple scaling arguments, the leading order scaling behavior of momentum relaxation rate $1/\tau_{\text{imp}}$ reads [6] :

$$\frac{1}{\tau_{\text{imp}}} \sim |V_{\text{imp}}|^2 T^{d+1-2/\nu}, \quad (38)$$

with random potential $V(r)$ coupling to $|z|^2$, and V_{imp} is defined as $\overline{V(r)V(r')} = V_{\text{imp}}^2 \delta^2(\vec{r} - \vec{r}')$. For a randomly distributed impurity with Yukawa potential $V_q =$

$V_z/(q^2 + \mu^2)$ and density n_{imp} , we can identify $V_{\text{imp}}^2 \sim n_{\text{imp}} V_z^2 / \mu^4$. Compensating the dimension by inserting the spinon bandwidth T_z and other physical constants, we obtain the equation for the thermal conductivity of spinons (Eq. 11 in the paper):

$$\kappa_z \sim \frac{Nc^2 \hbar k_B^4 \mu^4 T^2 T_z}{an_{\text{imp}} V_z^2} \times \left(\frac{T}{T_z} \right)^{2/\nu-3}. \quad (39)$$

Notice that this equation is only applicable to the case with $1/\tau_{\text{imp}} \ll T$.

III. THERMAL PROLIFERATION OF VISONS

In this section we discuss the regime $T > \Delta_v$, where the visons have thermally proliferated. As noted in the paper, at these temperatures the $1/T_1$ NMR relaxation rate is observed to have a plateau [5]. We believe this is a general feature of a dense vison regime: the presence of visons makes it harder for the spinons to propagate independently, and so a vector spin model (which has a T -independent NMR relaxation rate [4]) becomes more appropriate.

Here we will illustrate this qualitative idea in a specific model. Rather than thinking about this as high T regime for visons, imagine we reach this regime by sending $\Delta_v \rightarrow 0$ at fixed T . In other words, we are in the quantum critical region of a critical point where the vison gap vanishes leading to phase with the visons condensed. We have already argued in the paper that the spinons are also in the quantum critical region of a transition where the spinons condense. Thus a description of the spin dynamics in the regime $T > \Delta_v$ is provided by the quantum criticality of a multicritical point where both the spinons and visons condense. A general theory of such multicritical points has been discussed in a recent work by two of us. [2] The NMR relaxation is then given by $1/T_1 \sim T^{\eta_{mc}}$, where η_{mc} is the anomalous dimension of the magnetic order parameter at the spinon-vison

multicritical point.

Our only present estimates of η_{mc} come from the $1/N$ expansion, and so it is useful to compare estimates of anomalous dimensions in this expansion at different quantum critical points. For the regime, $T < \Delta_z$, discussed in the main paper, the NMR relaxation is controlled by the theory in Eq. (1) describing the condensation of the spinons alone. Here we have $1/T_1 \sim T^{\bar{\eta}}$ where [1]

$$\bar{\eta} = 1 + \frac{64}{3\pi^2 N}. \quad (40)$$

In the higher temperature regime, $T > \Delta_z$, we have $1/T_1 \sim T^{\eta_{mc}}$, and the same $1/N$ expansion for this exponent at the multicritical point where both spinons and visons condense yields [2]

$$\eta_{mc} = \bar{\eta} - \frac{256}{3\pi^2 N} \times \frac{1}{1 + 256k^2/(\pi^2 N^2)}. \quad (41)$$

Here k is the level of the Chern-Simons theory describing the multicritical point. The large N expansion is performed with k proportional to N , and the physical values are $k = 2$ and $N = 4$.

The key point is that $\eta_{mc} < \bar{\eta}$. Hence $1/T_1$ will have a weaker dependence on T for $T > \Delta_z$ than for $T < \Delta_z$.

-
- [1] A. V. Chubukov, T. Senthil and S. Sachdev, Phys. Rev. Lett. **72**, 2089 (1994).
 - [2] C. Xu and S. Sachdev, Phys. Rev. B **79**, 064405 (2009).
 - [3] C. Timm, S. M. Girvin, P. Henelius and A. W. Sandvik, Phys. Rev. B **58**, 1464 (1998).
 - [4] A. V. Chubukov, S. Sachdev, and J. Ye, Phys. Rev. B **49**, 11919 (1994).
 - [5] Y. Shimizu *et al.*, Phys. Rev. B **73**, 140407(R) (2006).
 - [6] S. A. Hartnoll *et al.*, Phys. Rev. B **76**, 144502 (2007); M. Müller and S. Sachdev, Phys. Rev. B **78**, 115419 (2008).